

# Experimental p-y loops for estimating seismic soil-pile interaction

Emmanouil Rovithis · Emmanouil Kirtas ·  
Kyriazis Pitilakis

Received: 17 April 2008 / Accepted: 7 April 2009 / Published online: 26 April 2009  
© Springer Science+Business Media B.V. 2009

**Abstract** Seismic soil-pile interaction is evaluated in this study based on back-calculated p-y loops constructed from sampled data of pile bending moments. Fundamental properties of p-y loops are implemented to derive distributed springs and dashpots, thereby quantifying soil-pile interaction in the realm of a Beam on Dynamic Winkler Foundation modeling. The procedure is validated by means of well-documented centrifuge tests of a single pile supported structure founded on a two-layer soil profile that comprises of soft clay overlying dense sand. Two shaking levels of a real earthquake motion applied at the base of the soil profile were examined and the generated seismic p-y loops were compared to cyclic p-y curves commonly used in pile design practice. The results demonstrate the strong influence of intensity of the input motion on seismic p-y loops while cyclic p-y curves established for soft clays tend to overestimate soil stiffness under strong excitation. Typical sets of recorded and computed structural response are presented, denoting the ability of the BDWF model related to p-y loops in reproducing adequately fundamental aspects of seismic soil-pile interaction.

**Keywords** Soil-pile-structure interaction · p-y loops · Centrifuge · Seismic response · Winkler model

## 1 Introduction

Design of piles against earthquake induced horizontal loads needs consideration of the interaction that takes place between pile and soil. Towards a computationally convenient analysis

---

E. Rovithis (✉) · E. Kirtas · K. Pitilakis  
Department of Civil Engineering, Aristotle University of Thessaloniki, P.O. Box 424,  
54124 Thessaloniki, Greece  
e-mail: rovithis@civil.auth.gr

E. Kirtas  
e-mail: kirtas@civil.auth.gr

K. Pitilakis  
e-mail: kpitilak@civil.auth.gr

of the soil-pile system, the Winkler method, where the soil is represented as a series of distributed springs attached to the pile shaft has been extensively utilized, reducing soil-pile interaction to a one-dimensional problem. The required spring stiffness is traditionally determined through nonlinear soil reaction-deflection curves, the so-called p-y curves. These p-y curves have been established for different soil conditions based on in-situ pile tests under static (monotonic) or cyclic pile-head loading (Matlock 1970; Cox et al. 1974; Reese et al. 1974, 1975; Murchinson and O'Neill 1984; Georgiadis et al. 1992; Reese 1997; Ashour and Norris 2000; Janoyan et al. 2001). Since the continuity condition in the soil is fully satisfied in field tests, the associated p-y curves constitute a direct representation of pile response under the particular types of loading, justifying their implementation in pile design procedures (API 1993).

Although the non-linear relationship between pile displacement and lateral soil reaction is accounted for, the p-y curves developed for monotonic or cyclic loading cannot adequately describe neither the reduction of soil stiffness with increasing amplitude of excitation, which is more pronounced for soft soil conditions, nor soil inertia effects that take place under dynamic loading (Angelides and Roesset 1981). Furthermore, material and wave radiation damping generated during pile oscillations affects substantially soil-pile interaction, modifying p-y relationship and introducing complex-valued dynamic soil stiffness as a function of the excitation frequency (Kagawa and Kraft 1980; Novak and El Sharnouby 1983; Gazetas and Dobry 1984; Nogami et al. 1992). Even though it has been reasoned that material non-linearity overshadows these frequency effects, this has not been verified by direct comparison of the static and dynamic lateral soil reactions (Ting et al. 1987).

In the realm of the Winkler approach, several models have been proposed for the analysis of seismic soil-pile interaction, including simplified relations of frequency dependent springs and dashpots (Dobry et al. 1982; Gazetas and Dobry 1984; Kavvadas and Gazetas 1993) for linear soil-pile systems as well as rigorous analytical p-y models (Matlock et al. 1978; Nogami et al. 1992; EL Naggari and Novak 1995, 1996; Badoni and Makris 1996; Boulanger et al. 1999; Gerolymos and Gazetas 2005; Gerolymos et al. 2007), where complex phenomena such as inelastic soil and pile response, soil-pile separation and/or sliding and soil stiffness or strength hardening (or degradation) can be adequately reproduced. These complex (though not rigorous) analytical models usually demand proper calibration of their parameters based on available experimental or numerical data (Gerolymos and Gazetas 2005).

In this paper, seismic soil-pile interaction is estimated through distributed pile springs and dashpots computed from p-y loops, which in turn are constructed from recorded pile bending moments, implementing simple beam theory. Disregarding potential soil-pile gapping and soil liquefaction, the scope of this study is twofold: (a) to examine the effect of intensity of the seismic excitation on p-y loops and consequently on pile and structural response and (b) to predict the seismic response of a coupled soil-pile-structure system by means of a Beam on Dynamic Winkler Foundation model, utilizing fundamental properties of the derived p-y loops. Well-documented centrifuge tests (Wilson et al. 1997; Wilson 1998; Boulanger et al. 1999) are employed to validate the proposed procedure while particular emphasis is placed on the simulation of recorded pile bending with pertinent interpolation functions.

## 2 Statement of the problem

Under static or cyclic pile-head loading the relation between pile displacement and lateral soil reaction is described through a non-linear p-y curve depending on the pile diameter, soil properties, depth below ground surface, geometric failure mechanism and level of water

table. Cyclic p-y curves deviate from the static ones when pile deflection reaches a limiting value due to the cyclic degradation of the soil. The static p-y curve proposed by Matlock (1970), for piles embedded in soft to medium clays is given by:

$$\frac{p}{P_{ult}} = 0.5 \left( \frac{y}{y_{50}} \right)^{1/3} \tag{1}$$

where  $p_{ult}$  represents the ultimate soil reaction and  $y_{50}$  the lateral pile deflection at one-half of the ultimate reaction. These parameters can be estimated by:

$$P_{ult} = c_u D_p N_p \tag{2}$$

$$N_p = \left( 3 + \frac{\gamma' z}{c_u} + \frac{Jz}{D_p} \right) \leq 9 \tag{3}$$

$$y_{50} = 2.5 D_p \epsilon_{50} \tag{4}$$

In the above expressions,  $D_p$  is the pile diameter,  $N_p$  the lateral bearing capacity factor,  $\gamma'$  the average buoyant unit weight,  $z$  the depth,  $c_u$  the undrained shear strength,  $\epsilon_{50}$  the strain corresponding to a stress of 50% of the ultimate stress in a laboratory stress-strain curve and  $J$  represents a constant term depending on the soil type (0.5 for soft clay and 0.25 for medium clay). According to Matlock’s recommendations, the depth  $z_{cr}$  at which the failure mechanism translates from wedge type near the ground surface to horizontal soil flow at greater pile depths equals to:

$$z_{cr} = \frac{6c_u D_p}{\gamma' D_p + Jc_u} \tag{5}$$

For cyclic loading the exponential form of the p-y curve, given by Eq. 1, is retained until a normalized pile displacement  $y/y_{50} = 3$ , where the soil reaction is considered as  $0.72P_{ult}$ , and then diminishes with increasing displacement for  $z < z_{cr}$  or remains constant for  $z > z_{cr}$ .

Under dynamic or seismic loading the force (per unit length of the pile)  $p$  to displacement  $y$  ratio of the Winkler medium at every depth, defines the complex-valued frequency-dependent impedance function (Novak 1974; Novak et al. 1978; Kavvadas and Gazetas 1993):

$$S_x = \frac{p}{y} = k_x(\omega) + i\omega c_x(\omega) \tag{6}$$

where the real part  $k_x(\omega)$  represents dynamic stiffness and the imaginary part  $\omega c_x(\omega)$  damping in the form of wave radiation and hysteretic action (material damping). Based on the above definition, various dynamic p-y curves have been proposed. Romo and Ovando-Shelley (1999) introduced a calibrated hyperbolic soil behavior model into the load-displacement relationship based on experimental data, while Bentley (1999) proposed an analytical dynamic p-y model by relating static p-y curves with excitation frequency. Along these lines, Hajjalilue-Bonab et al. (2007) obtained experimental p-y loops in dense sand, denoting their practical importance as a means for estimating dynamic soil springs in a Winkler model. This motivated the present study towards the formulation of a procedure for the evaluation of seismic soil-pile interaction, by correlating the dynamic soil stiffness, as represented by Eq. 6, with fundamental properties of p-y loops.

### 3 Outline of the proposed procedure

The procedure adopted in this study is described schematically in Fig. 1 (Rovithis 2007). Starting from a set of pile bending moments recorded under seismic excitation, one obtains

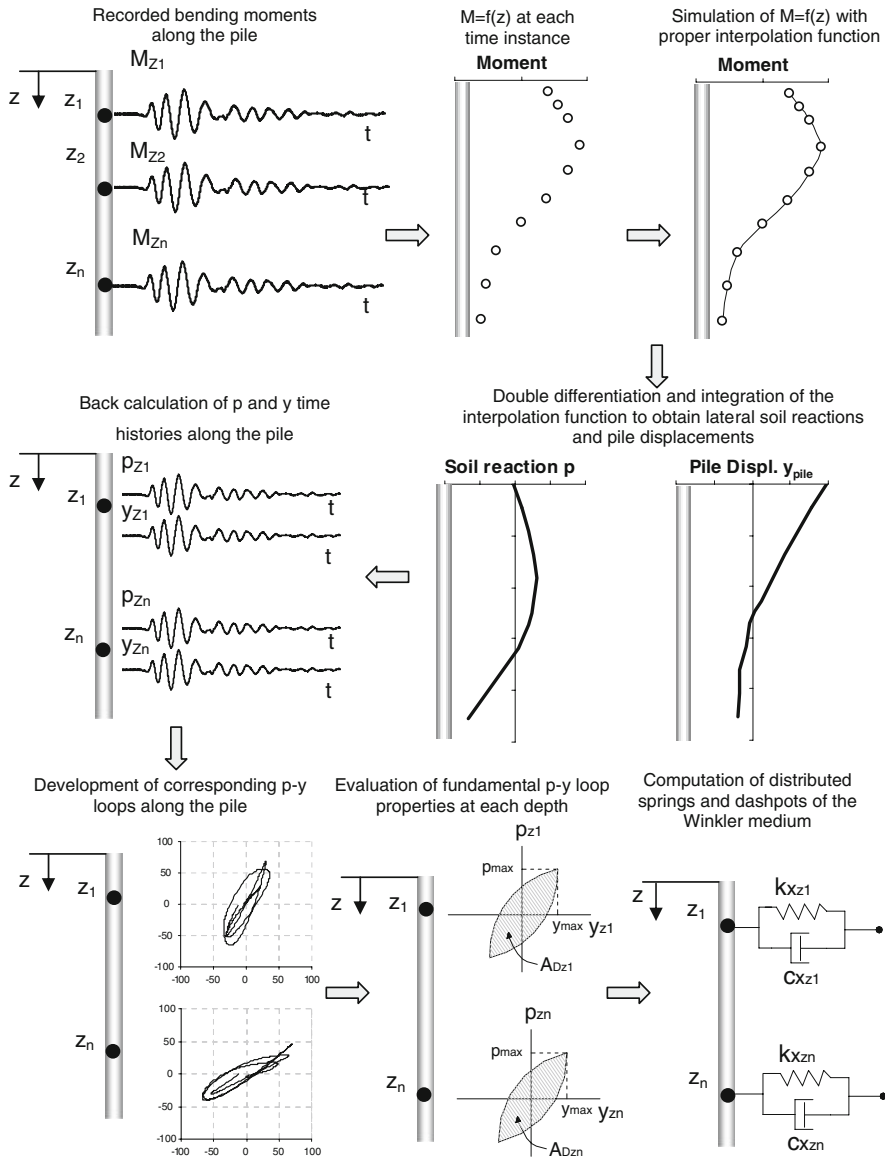


**Fig. 1** Overview of the proposed procedure

the distribution of pile moments, as a function of time and vertical distance  $z$  along the pile shaft. Therefore, for each time instance  $t_i$ , a different bending moment distribution  $M(z, t_i)$  is imposed on the pile. From elementary beam theory, the moment  $M(z, t_i)$  is proportional to the flexural strain  $\epsilon$  (Ting et al. 1987):

$$M(z, t_i) = E_p I_p \frac{d^2 y_{pile}}{dz^2} = E_p I_p \frac{\epsilon}{h} \tag{7}$$

where  $y_{pile}$  is the lateral pile deflection,  $z$  the vertical distance along the pile,  $h$  the distance from the gauge to the neutral axis of bending and  $E_p I_p$  the flexural stiffness of the pile section.

The bending moment  $M(z, t_i)$  is then double differentiated and integrated to calculate soil reaction  $p(z, t_i)$  and lateral pile deflection  $y_{pile}(z, t_i)$ :

$$p(z, t_i) = \frac{d^2 M(z, t_i)}{dz^2} \tag{8}$$

$$y_{pile}(z, t_i) = \frac{1}{E_p I_p} \int \int M(z, t_i) dz \tag{9}$$

The associated  $p$  and  $y_{pile}$  time histories along the pile shaft are then obtained by composing the lateral soil reaction  $p$  and pile displacement  $y_{pile}$  distributions computed at each time instance from Eqs. 8 and 9 respectively. For seismic loading, the relative displacement between pile and soil,  $y$ , is derived from  $y_{pile}$  after subtracting the free field soil deflected shape  $y_{soil}$ . Hence, back-calculated  $p$ - $y$  loops are generated along the pile, representing the seismic  $p$ - $y$  behavior. It should be mentioned that the soil reaction computed in this way does not include the dynamic pressure due to inertia of the pile element. However, it has been reasoned (Ting 1987) and experimentally verified (Hajjalilue-Bonab et al. 2007) that this dynamic pressure contribution is negligible with respect to the pressure computed from the beam theory and can therefore be neglected.

Fundamental properties of  $p$ - $y$  loops, namely the area  $A_D$  and slope of the loop are then determined by equating the area of the  $p$ - $y$  loop with the energy absorbed in one loading cycle for a viscously damped system excited harmonically. This leads to an estimate of the damping coefficient  $c_x(\omega)$ , according to the expression (Ting 1987):

$$c_x(\omega) = \frac{A_D}{\pi \omega y_{max}^2} \tag{10}$$

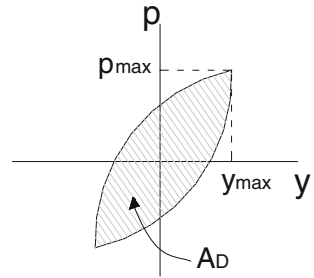
where  $\omega$  is the excitation frequency. Consequently, an equivalent viscous damping is derived from the seismic  $p$ - $y$  loop corresponding to the maximum displacement amplitude computed at each level along the pile shaft. The adopted approach represents actually an overall damping that is defined by the area of the seismic  $p$ - $y$  loop. Thus, the damping component of the proposed  $p$ - $y$  element includes both radiation and hysteretic damping, depending on the seismic motion characteristics and the soil properties. Accordingly, the associated slope of the seismic  $p$ - $y$  loop is defined as the ratio of the maximum soil reaction  $p_{max}$  to the respective lateral deflection  $y_{max}$ . Fig. 2 clarifies schematically the aforementioned  $p$ - $y$  loop characteristics. The real part  $k_x(\omega)$  may then be approximated by combining Eqs. 6 and 10, resulting in (Badoni and Makris 1996):

$$k_x(\omega) = \sqrt{\left(\frac{p_{max}}{y_{max}}\right)^2 - \left(\frac{A_D}{\pi y_{max}^2}\right)^2} \tag{11}$$

Thereby, seismic soil-pile interaction is quantified through stiffness and damping coefficients of the Winkler medium based on back-calculated  $p$ - $y$  loops.

Notwithstanding the approximation of the physical phenomenon that is introduced in the realm of a simplified BDWF model, the proposed procedure permits a realistic quantification of the dynamic soil-pile interaction that is compatible to the intensity level of the seismic motion. Apparently, in design practice the developed pile bending that constitute the required input data is not known beforehand. However, the implementation of the procedure for various seismic loadings (amplitude and frequency), soil conditions and pile characteristics

**Fig. 2** Schematic illustration of fundamental properties of a symmetric and perfectly closed p-y loop



could provide a basis towards an analytical prediction of springs and dashpots obtained from appropriate p-y loops.

### 3.1 Interpolation of pile bending moments

Since the bending moments data are known at discrete locations along the pile, a numerical scheme is necessary to describe the variation of recorded bending moments and obtain soil reactions and pile deflections. Two of the most commonly employed interpolation techniques involve fitting either cubic splines between successive data points (Scott 1980; Finn et al. 1983), or higher order polynomial functions to all data points (Ting et al. 1987, Meymand 1998). An alternative interpolation scheme has been proposed by Wilson (1998) based on minimizing weighted residuals. The selection of a proper interpolation function constitutes an important task, especially for the evaluation of soil reactions  $p(z, t_i)$ , since even a slight deviation in the recorded data becomes significantly magnified during the differentiation process (Ting 1987). Along these lines, it has been reasoned (Wallace et al. 2001) that the implementation of cubic splines may lead to non-physical, rapid fluctuations of the double differentiated fit function while continuous polynomial functions usually alleviate this problem, resulting in smoother variations of soil reaction.

#### 3.1.1 Validation of polynomial function under static pilehead loading

The ability of polynomial function to adequately reproduce lateral soil reactions was examined in this study by means of pile tests under static pile-head loading (Georgiadis et al. 1992). These centrifuge tests were performed at an acceleration level of 50 g (King et al. 1984), aiming at investigating the static p-y response of floating, steel piles embedded in uniform dry sand ( $D_r = 60\%$ ). The variation of bending moments imposed on two single piles under a static load equal to  $H = 997$  kN and  $H = 1304$  kN respectively was recorded by five pairs of strain gauges distributed along each pile. The piles had a common diameter  $D = 1$  m and length  $L = 9$  m while their flexural stiffness was slightly different ( $EI = 2,066$  and  $2,495$  MNm<sup>2</sup>).

A polynomial function was fitted to the recorded bending moments (Fig. 3a) and was compared to established results from the literature (Georgiadis et al. 1992). The order of the polynomial function was defined according to the number of the available data points. Since the bending moments were measured at five locations, almost evenly spaced, along the pile, a fourth order polynomial revealed adequate representation of pile response. Indeed, it is observed in Fig. 3, that the pile shear forces ( $S$ ), soil reaction ( $p$ ) and lateral pile deflection  $y_{\text{pile}}$  obtained, respectively, from the first derivative, second derivative and double integral of

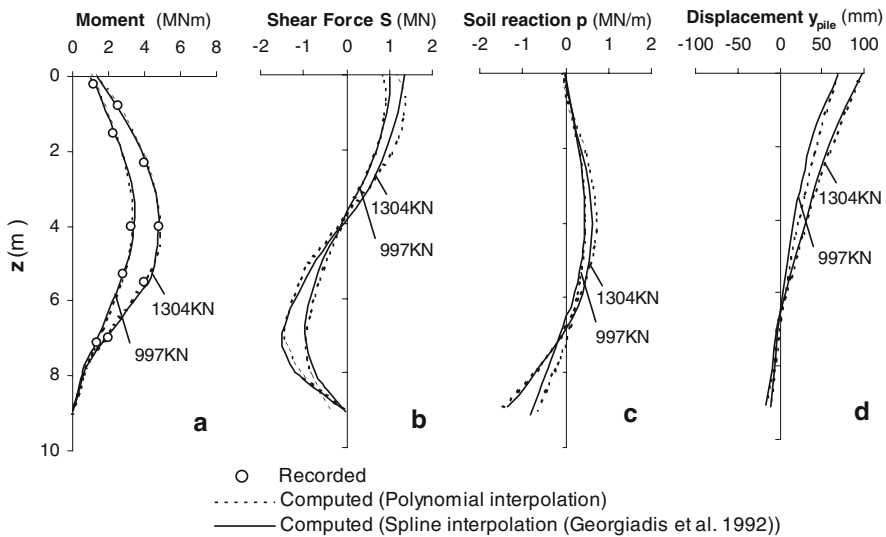


**Fig. 3** Comparison of polynomial and spline function for interpolating recorded pile bending moments developed under static pilehead loading

the polynomial function reproduce satisfactorily pile response, in agreement with the solution of Georgiadis et al. (1992).

#### 4 Seismic response of a soil-pile-structure system

A coupled soil-pile-structure system was subsequently analyzed by applying the proposed procedure on a series of well-documented dynamic centrifuge tests of a pile-supported structure on soft ground. Two shaking levels of a real earthquake excitation introduced at the base of the soil profile were examined to investigate the effect of intensity of seismic motion on  $p$ - $y$  loops. The generated  $p$ - $y$  loops were compared to cyclic  $p$ - $y$  curves commonly used in design practice and were then employed for the computation of dynamic soil stiffness. The seismic response of the coupled system is numerically obtained by means of a Beam on Dynamic Winkler Foundation model and analysis results are compared to the centrifuge recordings.

##### 4.1 Centrifuge experiments

The tests were performed in a 9-m-radius centrifuge at an acceleration level of 30  $g$  (Wilson et al. 1997, Wilson 1998; Boulanger et al. 1999). The inside dimensions of the centrifuge container are 1.7 m long, 0.7 m deep, and 0.7 m wide. The centrifuge model constitutes of a single pile supporting a SDOF structure founded on a soft clay layer overlying dense sand (Fig. 4). Specifically, the lower layer, in prototype scale, is a 11 m thick, dense Nevada sand layer with relative density  $D_r = 75$ –80%, while the upper is a 6 m thick clay layer of reconstituted Bay Mud with substantially low undrained shear strength. The height of the superstructure is equal to 4 m while its natural period under fixed-base conditions was measured at 0.29 s. The pile had a total length of 17 m and a flexural stiffness  $EI$  of 417  $MNm^2$ . The input motion

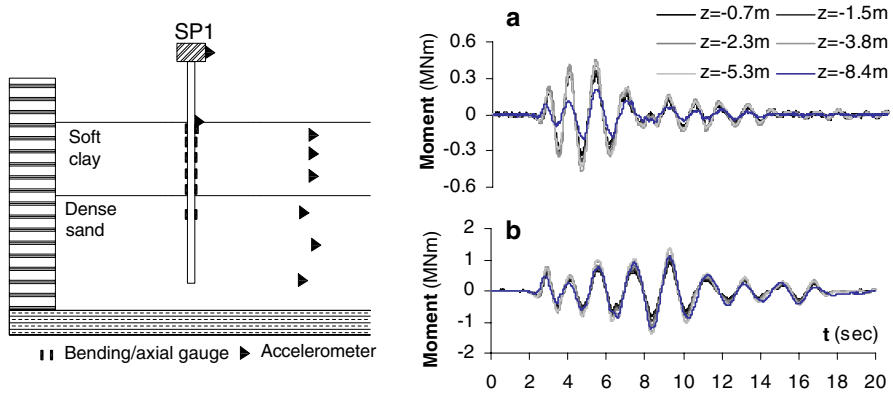


**Fig. 4** Configuration of the centrifuge model (after Boulanger et al. 1999) and pile bending moment recordings for **a** 0.05 g and **b** 0.20 g amplitude of the input motion

applied at the base of the soil profile is a strong motion accelerogram recorded in Port Island during the 1995 Kobe earthquake, scaled to a PGA of 0.05 g and 0.20 g respectively, covering a relatively wide range of shaking levels. Further details regarding the centrifuge apparatus as well as the soil and structural properties can be found in the aforementioned publications. Six pairs of bending/axial strain gauges (five in the soft clay layer and one in the dense sand layer) recorded the developed pile bending during the experiment. The instrumentation included also accelerometers attached to the pile-head, the superstructure mass as well as to various depths along the soil profile to record the free field soil response. Fig. 4 illustrates pile bending moments recorded at the locations of the strain gauges for each shaking level. To avoid high frequency noise during the differentiation process, these bending moment time histories were band pass filtered and were then utilized as input data to obtain back-calculated p-y loops.

#### 4.2 Derivation of p-y loops

Since the strain gauges were not evenly spaced along the pile, resulting in an insufficient sampling of bending moments at the lower part of the pile embedded in the sand layer, particular emphasis was placed on the effect of the polynomial function on the predicted pile response. Wilson (1998) performed a detailed investigation on the same centrifuge tests by interpolating bending moment profiles with three different methods (weighted residual method, cubic spline interpolation and polynomial interpolation). In his study three polynomial functions were examined, leading to the implementation of a non-integer five order polynomial as the most appropriate. Accordingly, three integer polynomial functions are studied herein, taking into consideration that bending moments were recorded at six locations along the pile and the polynomial order should not therefore be higher than five in order to ensure its uniqueness (Kiusalaas 2005). The effect of polynomial order on the variation of pile bending moments is depicted in Fig. 5, where the prediction of a third, fourth and fifth order polynomial is compared to the recorded data at indicative time instances, corresponding to peak recorded moments. Within the upper, highly instrumented portion of the pile, the results are practically insensitive to the degree of the polynomial, leading to an almost identical distribution of bending moments, in agreement with the centrifuge recordings. This verifies that closely spaced experimental data provides accurate predictions, regardless of the adopted interpola-

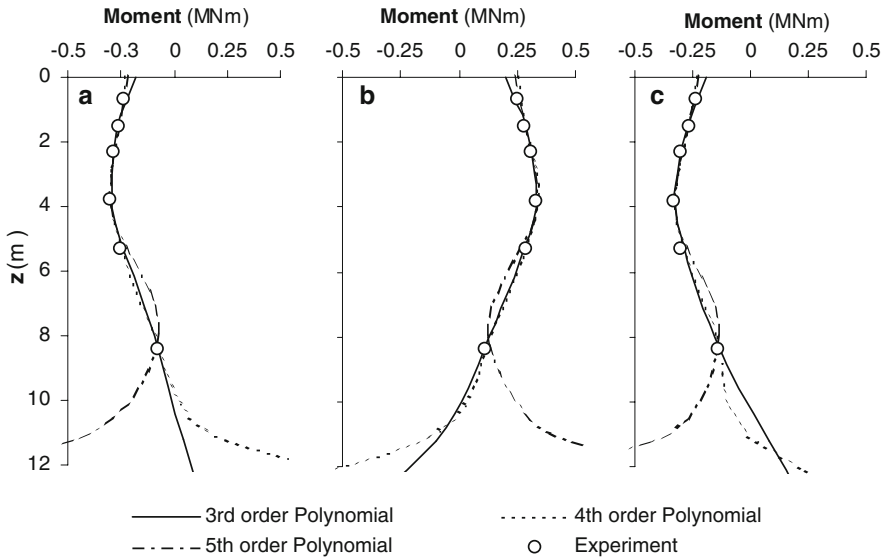


**Fig. 5** Effect of polynomial order on the interpolated bending moments recorded during the centrifuge test at **a**  $t = 4.62$  s **b**  $t = 5.275$  s and **c**  $t = 5.945$  s

tion method (Wilson 1998). On the other hand, within the lower part of the pile (i.e below the level of 6 m) where the recorded data is sparse, the variation of the bending moments presents a strong dependency on the degree of the polynomial. Particularly, it is observed that increasing the order of the polynomial results in unrealistically large values close to the pile tip. This abnormal distribution of bending moments associated with higher order polynomials was found to exist independently of the selected time instance. For this reason, a third order polynomial was finally adopted, providing the most reasonable approximation. Thus, the polynomial function  $M(z, t_i)$  utilized in the analysis of the particular centrifuge recordings is given by:

$$M(z, t_i) = A_{ti}z^3 + B_{ti}z^2 + C_{ti}z + D_{ti} \tag{12}$$

where the constant terms  $A_{ti}$ ,  $B_{ti}$ ,  $C_{ti}$ ,  $D_{ti}$ ,  $E_{ti}$  are defined for each time instance based on a least squares fit. Introducing the above polynomial in Eqs. 8 and 9 defines soil reaction ( $p$ ) and lateral pile displacement ( $y_{pile}$ ) distribution respectively.

During the integration procedure, two boundary conditions are required. The first one is determined at the pile head, where the displacement time history was calculated from the recorded acceleration. The second is obtained at the pile tip where the relative displacement between soil and pile was assumed to be zero, based on the high stiffness of the sand layer where pile deformations are expected to follow the displaced shape of soil. Thus, the second boundary condition was obtained by double integrating the soil acceleration time history recorded at this level. It is noted that various filtering techniques were implemented during the integration procedure of the acceleration recordings, based on the signal processing methods described by Wilson (1998). Mass-processing of the acceleration time histories included high-pass, low pass as well as band-pass Butterworth type filtering. It was observed that a band pass filter revealed minor deviation from the procedure proposed by Wilson and was thus implemented during the integration process of the acceleration recordings.

Typical results of computed seismic p-y loops for 0.05 g and 0.20 g amplitude of input motion are shown in Fig. 6a and 6b respectively. These p-y loops were obtained at 1.5 m, 3 m and 4.5 m within the soft clay layer and at 8.2 m within the underlying dense sand layer. Note that the p-y loops shown in Fig. 6 correspond to a specific time window of maximum p-y response (Meymand 1998). It is observed that the slope of p-y loops is increasing with depth, indicating higher soil stiffness, while the area is decreasing, denoting lower levels of damping during pile oscillations. This is further established in Fig. 7 where the p-y loops generated at  $z=3$  m and  $z=4.5$  m are compared to the results of Wilson (1998) computed at the depth of  $z=5.14$  m. Indeed, at this greater depth the slope of the p-y loop is further increased and the area is accordingly decreased, leading to comparable p-y loops. The observed p-y response should be correlated with the reduction of lateral pile deflections with depth and the associated linear response prevailing over the nonlinear hysteretic action in the soil (Hajjalilue-Bonab et al. 2007).

Of particular interest is the modification of the p-y loops with increasing intensity of the excitation. Focusing on the p-y loops generated within the soft clay layer (i.e.  $z=1.5$ , 3 and 4.5 m) it is observed that for 0.20 g, strong nonlinear hysteretic behavior is mobilized as opposed to the p-y response for the low amplitude (0.05 g) motion, where the soil response remains essentially in the linear range. Thus, increasing the intensity of excitation results in substantially softer p-y loops (i.e. smaller p-y slope) and significantly higher levels of damping (i.e. larger p-y loop area).

#### 4.2.1 Comparison with cyclic p-y curves

Cyclic p-y curves based on API (1993) are also shown in Fig. 6 with dashed lines. More specifically, the generated p-y curves within the soft clay layer correspond to Matlock's cyclic model, as computed by Eqs. 1–5. The variable  $\epsilon_{50}$  was taken equal to 0.005 based on published laboratory test data for this particular soil type (Boulanger et al. 1999) while parameter J was selected equal to 0.5 according to Matlock's recommendations for soft clay. For the underlying dense sand layer, the p-y curve proposed by Murchison and O'Neill (1984) was adopted. Soil layering revealed minor effect on the p-y curves and the associated structural seismic response (Boulanger et al. 1999) and was therefore neglected herein.

For particularly soft clay, as the one tested in the centrifuge, it is observed that for the low amplitude motion, the initial part of the cyclic p-y curve is in agreement with the slope of the generated p-y loops, providing an adequate estimate of the spring stiffness and leading to comparable maximum lateral soil reactions. On the contrary, for higher levels of excitation (0.20 g), the cyclic model tends to overestimate soil stiffness, resulting in substantially stiffer p-y curves. Apparently, the damping reflected by the area of the p-y loop under seismic motion cannot be reproduced by analytical p-y curves that have been established for cyclic pilehead loading. This deviation may be of importance in design when piles embedded in soft soil deposits are subjected in strong ground motion.

#### 4.3 Numerical analysis utilizing a BDWF model

The seismic response of the examined soil-pile-structure system was analyzed with the general-purpose FE code ANSYS (2000), implementing a Beam on Dynamic Winkler Foundation model (Fig. 8). The pile-structure system was modeled with linear elastic beam elements and each pile node was directly connected to a Kelvin element. Note that seismic p-y loops were obtained at the specific locations along the pile where the free field response was recorded by the vertical array installed within the soil profile. Thus, soil displacement time

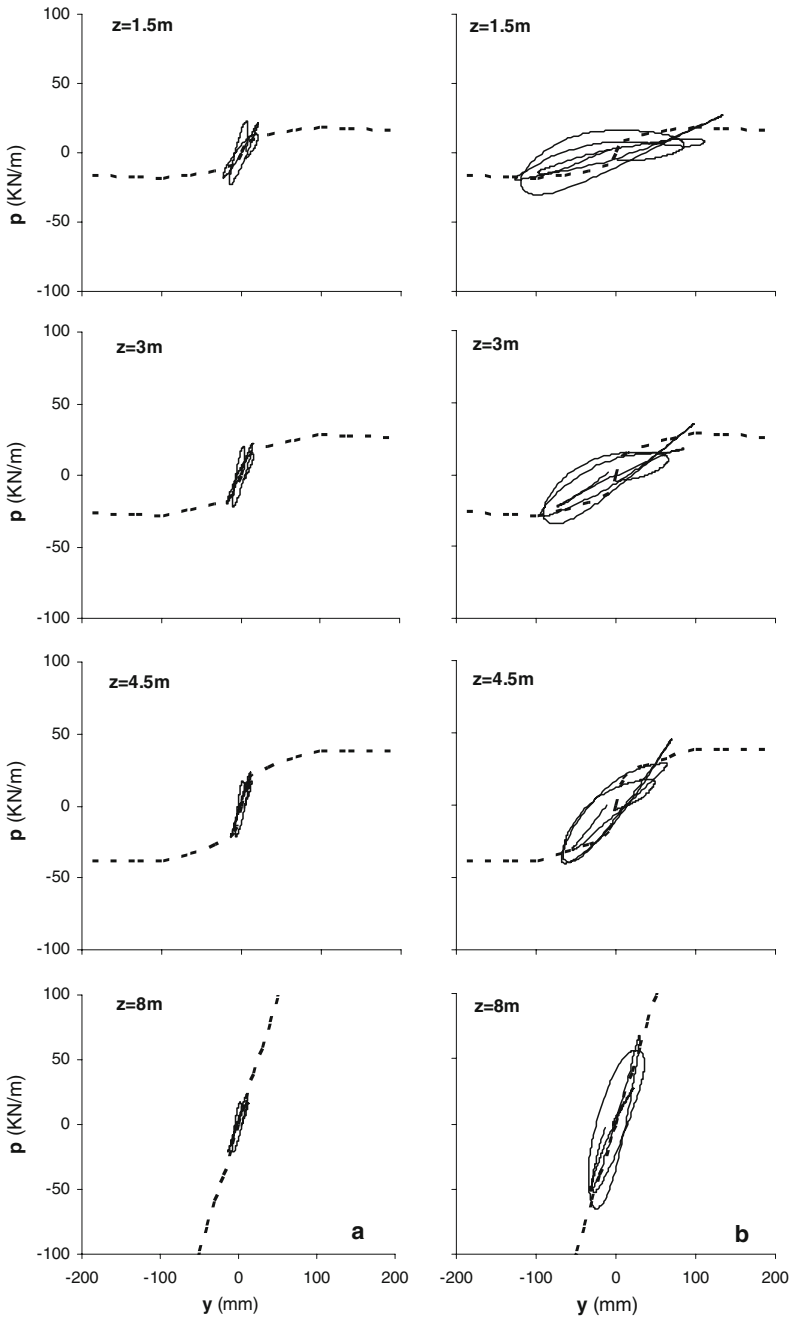


**Fig. 6** Seismic  $p$ - $y$  loops generated along the pile shaft for **a** 0.05 g and **b** 0.20 g amplitude of the input motion. Comparison with cyclic  $p$ - $y$  curves (dashed lines) commonly used in design practice API (1993)

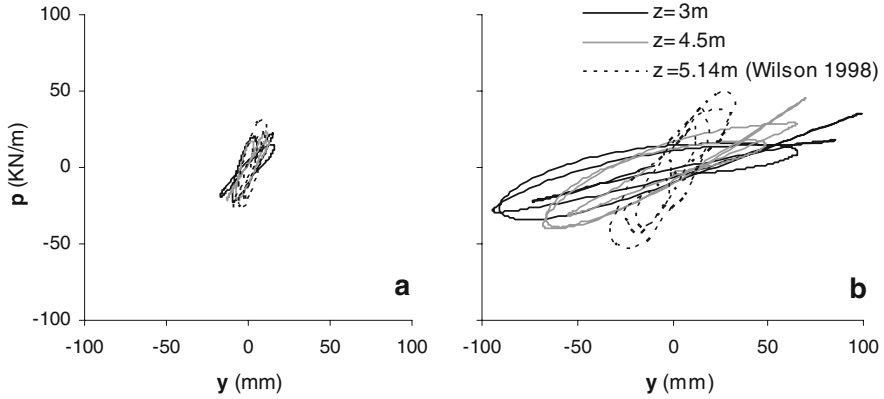
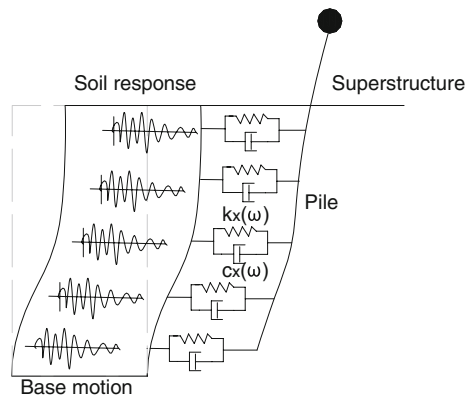


**Fig. 7** Comparison of the p-y loops at the depth of  $z = 3$  m and  $z = 4.5$  m with the p-y loops computed by Wilson (1998) at the depth of  $z = 5.14$  m for **a** 0.05 g and **b** 0.20 g seismic event

**Fig. 8** Beam on Dynamic Winkler Foundation model of the examined soil-pile-structure system (modified after Boulanger et al. 1999)



histories obtained by filtering and double integrating the recorded acceleration time histories were directly imposed at the ends of the Kelvin elements as the input motion. Mention has been already made regarding the filtering schemes that were adopted during the integration procedure. Utilizing recorded free field motions reduces the level of uncertainty related to the selection of appropriate ground parameters in a site response analysis. Any deviation between computed and recorded pile and structural response can therefore be attributed to the dynamic p-y analyses (Boulanger et al. 1999).

The real and imaginary part of the complex-valued impedance function  $S_x$  Eq. 6 is frequency dependent only through the properties of the seismic p-y loop, namely the area  $A_D$  and the slope of the loop. However, the Kelvin elements assigned in the BDWF model demand the evaluation of stiffness and damping coefficients,  $k_x$  and  $c_x$  respectively. In order to characterize the frequency content of the input motion with a single parameter and thus calculate the required stiffness and damping components from Eqs. 10 and 11, two simplified approaches were examined. The first corresponds to the predominant frequency  $f_o$  of the seismic motion that defines the frequency at which the Fourier spectra reaches its maximum value (Makris et al. 1993). The second one deals with the evaluation of a mean frequency  $f_m$ , which averages frequencies in the Fourier amplitude spectrum and weights each frequency by the square of its Fourier amplitude (Rathje et al. 1998):

$$f_m = \frac{\sum_i C_i^2 f_i}{\sum_i C_i^2}, \quad 0.25 \text{ Hz} \leq f_i \leq 20 \text{ Hz} \tag{13}$$

where  $C_i$  represents the Fourier amplitudes and  $f_i$  the discrete frequencies of the Fourier spectrum between 0.25 and 20 Hz. These frequency content parameters were evaluated based on the Fourier spectra (Fig. 9) of the accelerations recorded in the free field array for each shaking level of base excitation. Figure 10a shows the distribution of these characteristic frequencies along the soil profile. It is worth mentioning that increasing the amplitude of base motion shifts the frequency content of the free field response to lower frequencies, indicating an associated decrease in soil stiffness, especially within the upper soft clay layer.

Comparative analyses of the examined soil-pile-structure system revealed that the utilization of the predominant frequency  $f_0$  resulted in the most accurate prediction of the recorded

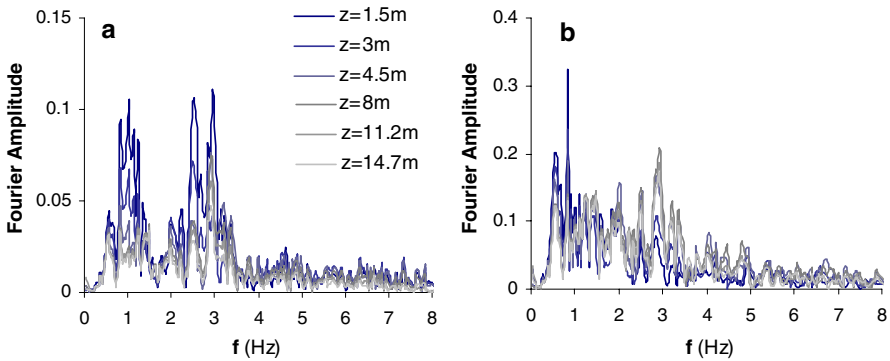


**Fig. 9** Fourier spectra of the free field accelerations recorded within the soil profile for **a** 0.05 g and **b** 0.20 g amplitude of the input motion

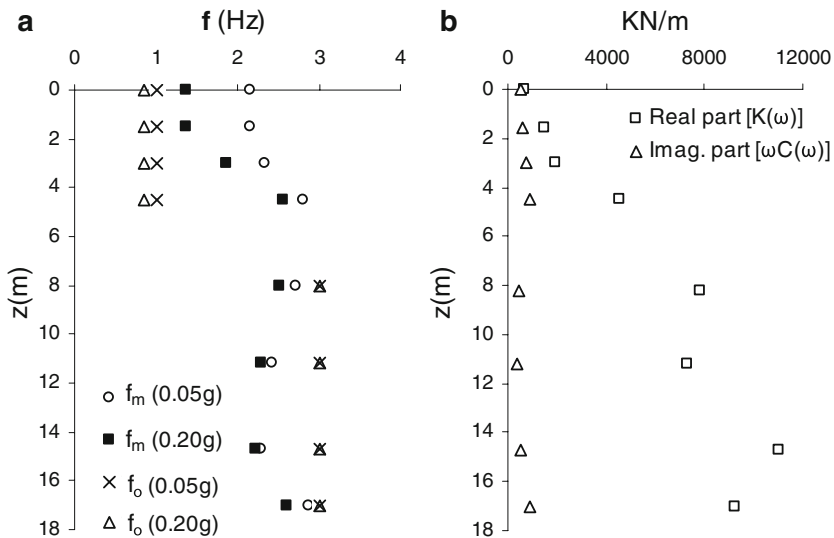


**Fig. 10** **a** Predominant frequency ( $f_0$ ) and mean frequency ( $f_m$ ) estimates based on free field centrifuge recordings for each shaking level of the base excitation **b** Distribution of real and imaginary part of the soil impedance function based on back-calculated p-y loops for the low amplitude (0.05 g) base motion

response and was thus considered as the single parameter that describes the frequency content of the input motion. Indicative results of the real and imaginary part of the soil impedance function obtained along the pile shaft are depicted in Fig. 10b, corresponding to the low amplitude (0.05 g) base excitation.

#### 4.3.1 Typical sets of recorded and computed response

Having determined the distributed springs and dashpots as well as the free field input motion, the proposed BDWF model was analyzed for each shaking level of base excitation and the computed seismic response was compared to the centrifuge recordings. Typical sets of recorded and computed response are presented in Figs. 11–14 concerning both pile and structural response.

In time domain, the computed pilehead and superstructure response (Figs. 11–12) follows closely the recorded motion, reproducing peak acceleration amplitude and frequency content of motion. However, for higher levels of base excitation (0.20 g, Fig. 12), the computed response presents a smooth attenuation in time, resulting actually in a harmonic type of motion with a dominant period close to 2 s. On the contrary, centrifuge recordings are characterized by lower amplitudes at the end of the shaking. This deviation of recorded and computed response, which is also observed in the peak spectral accelerations (Fig. 13) could probably be the result of a more complicated soil response including substantial variations of the p-y loops properties during the seismic event, radiation damping mechanisms or phenomena related to centrifuge testing modeling (e.g. “box” effect), which apparently cannot be fully reproduced with a simplified BDWF model, as the one adopted in the present study.

Of particular interest is the effect of intensity of the base excitation on the vibrational characteristics of the system, the magnitude of lateral displacement sustained by the structure, as well as on the bending moments imposed on the single pile. Based on the acceleration response spectra obtained for 0.05 g and 0.20 g respectively (Fig. 13), it is observed that increasing shaking level shifts the peak spectral acceleration to higher periods, indicating a dominant role of soil compliance on the effective (SSI) natural period of the system. Moreover, substantial increase of both the peak lateral deflections and pile bending moments (Fig. 14) was recorded for the strongest shaking event, resulting in considerably higher values than the ones recorded for the low amplitude motion. Notwithstanding the sharp soil stiffness contrast at the level of the clay-sand interface ( $z=6$  m), the peak bending moment occurs

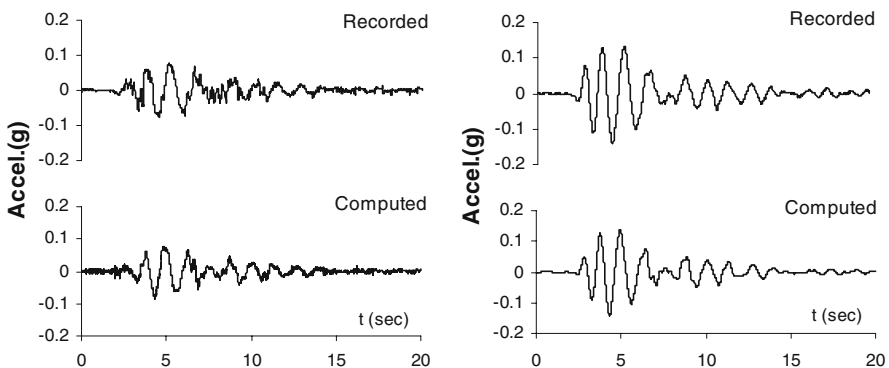


**Fig. 11** Recorded and computed accelerations at pilehead (*left*) and superstructure (*right*) for 0.05 g amplitude of the input motion

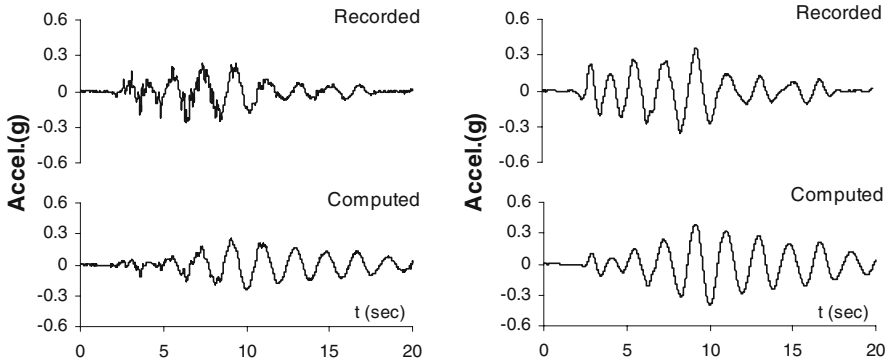


**Fig. 12** Recorded and computed accelerations at pilehead (*left*) and superstructure (*right*) for 0.20 g amplitude of the input motion

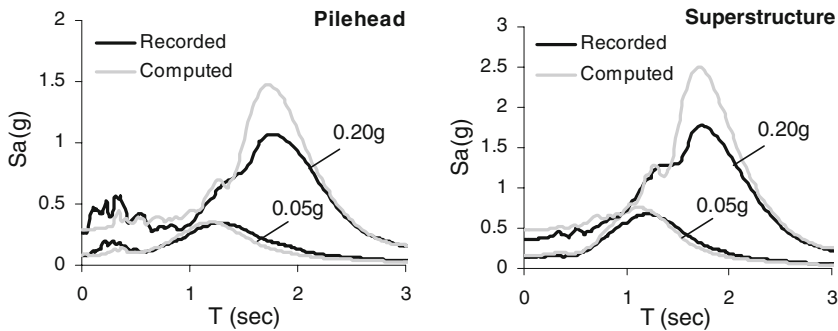


**Fig. 13** Recorded and computed acceleration response spectra at pilehead (*left*) and superstructure (*right*)

close to the pilehead. This should be attributed to inertial loading transmitted directly to the single pile foundation as a shear force and bending moment during superstructure oscillations (Mylonakis et al. 1997; Wilson 1998). Note also that the depth where the maximum bending moment occurs increases with increasing peak base acceleration. Similar findings have been reported by Boulanger et al. (1999). The aforementioned soil-pile-structure interaction effects are well captured by the adopted BDWF model, providing a strong experimental verification of the proposed procedure over a relatively wide range of shaking levels.

### 5 Conclusions

An integrated procedure for estimating seismic soil-pile interaction by means of p-y loops was formulated based on the Winkler approach for modeling dynamic stiffness of soil. Notwithstanding the complexity of the interaction mechanism, the proposed method resulted in a simplified yet sufficiently accurate evaluation of distributed pile springs and dashpots that may be utilized to predict the seismic response of pile-supported structures. The main conclusions can be summarized as follows:

- The utilization of continuous polynomial functions for interpolating recorded pile bending moments leads to a sufficiently accurate prediction of p-y response, given that reliable and closely spaced experimental data are available.

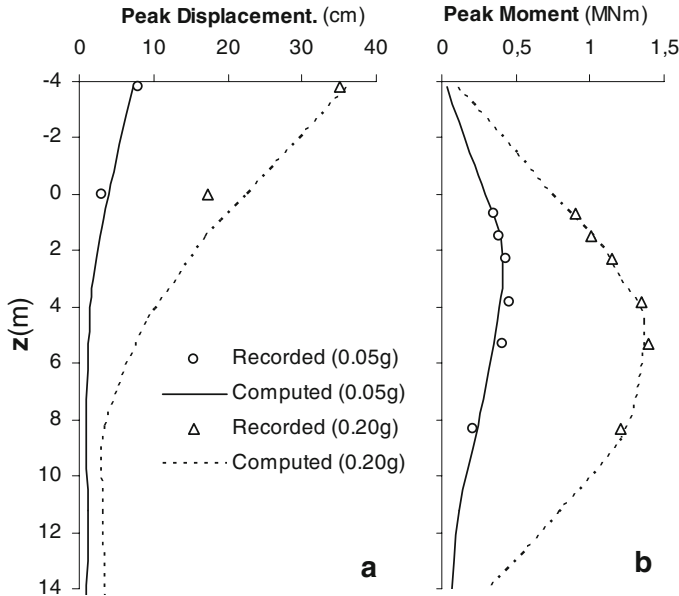


**Fig. 14** Recorded and computed peak lateral deflections and pile bending moments: **a** Peak absolute displacements **b** Peak bending moments

- The intensity of seismic excitation possesses a dominant role on p-y response, modifying the associated p-y loops, especially for soft soil conditions. Relatively high levels of shaking (e.g 0.20 g) mobilized significant non-linear hysteretic action in the supporting soil. In this case, particularly soft p-y loops were generated accompanied with high levels of damping, as opposed to the essentially linear soil response that was observed for lower amplitudes (0.05 g) of input motion.
- Existing cyclic models that have been established for soft clays tend to overestimate soil stiffness under relatively strong ground motion, resulting in stiffer p-y curves compared to the actual p-y seismic response.
- Utilizing p-y loops as a means for estimating seismic soil-pile interaction was validated using experimental data, providing a direct and reliable measure of soil stiffness and damping. Thus, the use of additional physical test data for various soil-pile-structure configurations and different seismic excitations may lead to an analytical evaluation of distributed pile springs and dashpots based on p-y loops, denoting a potential implication of the proposed procedure in pile design practice.

It is worth to mention that the present study was based on the assumptions of single pile foundation and perfect bonding between soil and pile. Consequently, the above conclusions may not be valid when geometrical nonlinearities (i.e. soil-pile separation and/or sliding) or strong pile group effects are activated.

**Acknowledgment** The first author would like to acknowledge the contribution of IKY foundation.

## References

- Angelides DC, Roesset JM (1981) Nonlinear lateral dynamic stiffness of piles. *J Geotech Eng Div* 107(No GT11):1443–1460
- ANSYS Inc (2000) ANSYS User's manual Version. 8.1. SAS IP Houston, USA

- API (1993) Recommended practice for planning, designing and constructing fixed offshore platforms. API RP 2A-WSD. 20. American Petroleum Institute, Washington, DC
- Ashour M, Norris G (2000) Modelling lateral soil-pile response based on soil-pile interaction. *J Geotech Geoenviron Eng* 126(5):420–428. doi:[10.1061/\(ASCE\)1090-0241\(2000\)126:5\(420\)](https://doi.org/10.1061/(ASCE)1090-0241(2000)126:5(420))
- Badoni D, Makris N (1996) Nonlinear response of single piles under lateral inertial and seismic loads. *Soil Dyn Earthq Eng* 15:29–43. doi:[10.1016/0267-7261\(95\)00027-5](https://doi.org/10.1016/0267-7261(95)00027-5)
- Bentley KJ (1999) Lateral response of piles under extreme events. MSc thesis. Department of Civil and Environmental Engineering, University of Western Ontario, London, Ontario
- Boulanger RW, Curras CJ, Kutter BL, Wilson DW, Abghari A (1999) Seismic soil-pile-structure interaction experiments and analyses. *J Geotech Geoenviron Eng* 125(9):750–759. doi:[10.1061/\(ASCE\)1090-0241\(1999\)125:9\(750\)](https://doi.org/10.1061/(ASCE)1090-0241(1999)125:9(750))
- Cox WR, Reese LC, Grubbs BR (1974) Field testing of laterally loaded piles in sand. In: Proceedings of the 6th offshore technology conference, Houston, Texas, Paper OTC 2079
- Dobry R, Vicente E, O'Rourke MJ, Roesset JM (1982) Horizontal stiffness and damping of single piles. *J Geotech Eng Div* 108(No.GT3):439–459
- EL Naggar MH, Novak M (1995) Nonlinear lateral interaction in pile dynamics. *Soil Dyn Earthq Eng* 14:141–157. doi:[10.1016/0267-7261\(94\)00028-F](https://doi.org/10.1016/0267-7261(94)00028-F)
- EL Naggar MH, Novak M (1996) Nonlinear analysis for dynamic lateral pile response. *Soil Dyn Earthq Eng* 15:233–244. doi:[10.1016/0267-7261\(95\)00049-6](https://doi.org/10.1016/0267-7261(95)00049-6)
- Finn WDL, Barton YO, Towhata I (1983) Seismic response of offshore pile foundations. In: Proceedings of the 7th Pan-American conference on soil mechanics and foundation engineering, Vancouver
- Gazetas G, Dobry R (1984) Horizontal response of piles in layered soils. *J Geotech Eng* 110(1):20–40. doi:[10.1061/\(ASCE\)0733-9410\(1984\)110:1\(20\)](https://doi.org/10.1061/(ASCE)0733-9410(1984)110:1(20))
- Georgiadis M, Anagnostopoulos C, Safflekou S (1992) Centrifugal testing of laterally loaded piles in sand. *Can Geotech J* 29:208–216
- Gerolymos N, Gazetas G (2005) Phenomenological model applied to inelastic response of soil-pile interaction systems. *Soil Found* 45(4):119–132
- Gerolymos N, Drosos V, Escoffier S, Gazetas G, Garnier J (2007) Numerical modeling of centrifuge cyclic lateral pile load experiments. In: Proceedings of the 2nd Greece-Japan workshop on seismic design, observation and Retrofit of foundations, Tokyo, Japan, pp 299–319, 3–4 April
- Hajjalilue-Bonab M, Levacher D, Chazelas JL (2007) Experimental evaluation of static and dynamic p-y curves in dense sand. In: Proceedings of the 4th international conference on earthquake geotechnical engineering, Thessaloniki, Greece, paper No.1696, 25–28 June
- Janoyan K, Stewart JP, Wallace JW (2001) Analysis of p-y curves from lateral load test of large diameter drilled shaft in stiff clay. In: Proceedings of the 6th Caltrans workshop on seismic research, Sacramento, CA
- Kagawa T, Kraft LM (1980) Seismic p-y responses of flexible piles. *J Geotech Eng Div* 106(GT84):899–918
- Kavvasdas M, Gazetas G (1993) Kinematic seismic response and bending of free-head piles in layered soil. *Geotechnique* 43(2):207–222
- King GJW, Dickin EA, Lyndon A (1984) The development of a medium-size centrifugal testing facility. In: Proceedings of the symposium on application of centrifuge modeling to geotechnical design, Manchester, UK, pp 25–45
- Kiusalaas J (2005) Numerical methods in engineering with MATLAB. Cambridge University press, Cambridge
- Makris N, Badoni D, Delis E, Gazetas G (1993) Prediction of observed bridge response with soil-pile-structure interaction. *J Struct Eng* 120(10):2992–3011. doi:[10.1061/\(ASCE\)0733-9445\(1994\)120:10\(2992\)](https://doi.org/10.1061/(ASCE)0733-9445(1994)120:10(2992))
- Matlock H (1970) Correlations for design of laterally loaded piles in soft clay. In: Proceedings of the 2nd annual offshore technology conference, vol 1, Houston, Texas, pp 577–594
- Matlock H, Foo SH, Bryant LL (1978) Simulation of lateral pile behaviour. In: Proceedings earthquake engineering and soil dynamics, ASCE, New York, pp 600–619
- Meymand PH (1998) Shaking table scale model tests of nonlinear soil-pile-superstructure interaction in soft clay. PhD Thesis, University of California, Berkeley
- Murchinson JM, O'Neill MW (1984) Evaluation of p-y relationships in cohesionless soils. In: Meyer JR (ed) Analysis and design of pile foundations. ASCE, New York, pp 174–191
- Mylonakis G, Nikolaou A, Gazetas G (1997) Soil-pile-bridge seismic interaction: kinematic and inertial effects. Part I: soft soil. *Earthq Eng Struct Dyn* 26:337–359. doi:[10.1002/\(SICI\)1096-9845\(199703\)26:3<337::AID-EQE646>3.0.CO;2-D](https://doi.org/10.1002/(SICI)1096-9845(199703)26:3<337::AID-EQE646>3.0.CO;2-D)
- Nogami T, Otani J, Konagai K, Chen H (1992) Nonlinear soil-pile interaction model for dynamic lateral motion. *J Geotech Eng* 118(1):89–106. doi:[10.1061/\(ASCE\)0733-9410\(1992\)118:1\(89\)](https://doi.org/10.1061/(ASCE)0733-9410(1992)118:1(89))
- Novak M (1974) Dynamic stiffness and damping of piles. *Can Geotech J* 11(4):574–598. doi:[10.1139/t74-059](https://doi.org/10.1139/t74-059)

- Novak M, El Sharnouby B (1983) Stiffness constants of single piles. *J Geotech Eng* 109(7):961–974. doi:[10.1061/\(ASCE\)0733-9410\(1983\)109:7\(961\)](https://doi.org/10.1061/(ASCE)0733-9410(1983)109:7(961))
- Novak M, Nogami T, Aboul-Ella F (1978) Dynamic soil reactions for plane strain case. *J Eng Mech Div* 104(4):953–959
- Rathje EM, Abrahamson NA, Bray JD (1998) Simplified frequency contents estimates of earthquake ground motions. *J Geotech Geoenviron Eng* 124(2):150–158. doi:[10.1061/\(ASCE\)1090-0241\(1998\)124:2\(150\)](https://doi.org/10.1061/(ASCE)1090-0241(1998)124:2(150))
- Reese LC (1997) Analysis of laterally loaded piles in weak rock. *J Geotech Geoenviron Eng* 123(11):1010–1017. doi:[10.1061/\(ASCE\)1090-0241\(1997\)123:11\(1010\)](https://doi.org/10.1061/(ASCE)1090-0241(1997)123:11(1010))
- Reese LC, Cox WR, Koop FD (1974) Analysis of laterally loaded piles in sand. In: Proceedings of the 6th offshore technology conference, Paper 2080, Houston, Texas, pp 473–483
- Reese LC, Welch RC (1975) Lateral loading of deep foundation in stiff clay. *J Geotech Eng Div* 101(7):633–649
- Romo MP, Ovando-Shelley E (1999) P-Y curves for piles under seismic lateral loads. *Geotech Geol Eng* 16:251–272. doi:[10.1023/A:1008859824440](https://doi.org/10.1023/A:1008859824440)
- Rovithis E (2007) Dynamic analysis of coupled soil-pile-structure systems. PhD Thesis (in Greek with English abstract). Department of Civil Engineering, Aristotle University of Thessaloniki, Thessaloniki
- Scott RF (1980) Analysis of centrifuge pile tests; simulation of pile-driving. Report for the American Petroleum Institute OSAPR Project 13, California
- Ting JM (1987) Full-scale cyclic dynamic lateral pile response. *J Geotech Eng* 113(1):30–45. doi:[10.1061/\(ASCE\)0733-9410\(1987\)113:1\(30\)](https://doi.org/10.1061/(ASCE)0733-9410(1987)113:1(30))
- Ting JM, Kauffman CR, Lovicsek M (1987) Centrifuge static and dynamic lateral pile behaviour. *Can Geotech J* 24:198–207
- Wallace JW, Fox PJ, Stewart JP, Janoyan K, Qiu T, Lermite S (2001) Cyclic large deflection testing of shaft bridges, Part I: Background and field test results. Research Report, Department of Civil and Environmental Engineering, University of California, Los Angeles
- Wilson DW (1998) Soil-pile-superstructure interaction in liquefying sand and soft clay. PhD Thesis, Department of Civil and Environmental Engineering, University of California, Davis
- Wilson DW, Boulanger RW, Kutter BL (1997) Soil-pile-superstructure interaction at soft or liquefiable soil sites—Centrifuge data report for Csp4. Rep. No UCD/CGMDR-97/05 center for geotechnical modeling, Department of Civil and Environmental Engineering, University of California, Davis